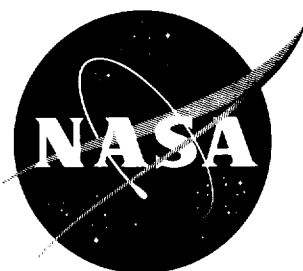NASA TN D-391

TECHNICAL NOTE

D-391

THE INFLUENCE OF LOW WALL TEMPERATURE ON

BOUNDARY-LAYER TRANSITION AND LOCAL HEAT TRANSFER ON

2-INCH-DIAMETER HEMISPHERES AT A MACH NUMBER OF 4.95

AND A REYNOLDS NUMBER PER FOOT OF 73.2×10^6

By Morton Cooper, Edward E. Mayo, and Jerome D. Julius

Langley Research Center
Langley Field, Va.

NATIONAL AERONAUTICS AND SPACE ADMINISTRATION

WASHINGTON   July 1960

L
7
5
2

NATIONAL AERONAUTICS AND SPACE ADMINISTRATION

TECHNICAL NOTE D-391

THE INFLUENCE OF LOW WALL TEMPERATURE ON

BOUNDARY-LAYER TRANSITION AND LOCAL HEAT TRANSFER ON

2-INCH-DIAMETER HEMISPHERES AT A MACH NUMBER OF 4.95

AND A REYNOLDS NUMBER PER FOOT OF 73.2×10^6

By Morton Cooper, Edward E. Mayo, and Jerome D. Julius

SUMMARY

Measurements of the location of boundary-layer transition and the local heat transfer have been made on 2-inch-diameter hemispheres in the Langley gas dynamics laboratory at a Mach number of 4.95, a Reynolds number per foot of 73.2×10^6, and a stagnation temperature of approximately 400° F. The transient-heating thin-skin calorimeter technique was used, and the initial values of the wall-to-stream stagnation-temperature ratios were 0.16 (cold-model tests) and 0.65 (hot-model test).

During two of the four cold tests, the boundary-layer flow changed from turbulent to laminar over large regions of the hemisphere as the model heated. On the basis of a detailed consideration of the magnitude of roughness possibly present during these two cold tests, it appears that this destabilizing effect of low wall temperatures (cooling) was not caused by roughness as a dominant influence. This idea of a decrease in boundary-layer stability with cooling has been previously suggested. (See, for example, NASA Memorandum 10-8-58E.) For the laminar data obtained during the early part of the hot test, the correlation of the local-heating data with laminar theory was excellent.

INTRODUCTION

Considerable interest has been stimulated in the problem of boundary-layer transition on blunt bodies in hypersonic flows for the following reasons: First, the ability to predict transition means the ability to make optimum, from heat-transfer considerations, blunt-body design for reentry shapes; and second, the transition problem on blunt bodies appears to be different in mechanism from that predicted by classical laminar-stability theory (ref. 1), which has proved, qualitatively, so satisfactory

for slender bodies. Unlike the slender-body case, cooling on blunt bodies appears to have a destabilizing effect. (The term "blunt body" is restricted in this discussion to mean only the nose (high curvature) region of the body and does not include any afterbody which may exist.) In fact transition data for hemispheres, obtained from many sources, have been "correlated" (refs. 2 and 3) to indicate the destabilizing influence of cold walls. These "correlations," however, even as pointed out in references 2 and 3, leave much to be desired. From a practical viewpoint this cooling problem is of importance at hypersonic speeds because the boundary layer around all very high Mach number vehicles will be cooled in the sense that there will be a heat flow from the boundary layer to the body.

The theoretical status of the problem rests primarily on qualitative discussions. For the blunt body it is agreed (refs. 4 to 6) that cooling is destabilizing on flows over convex surfaces. However, according to references 4 and 5, the stabilizing effect of the increasing angular momentum of the fluid in the outward direction is always greater than the destabilizing effect introduced by the low wall temperature (high local density). This phenomenon would imply a higher transition Reynolds number for a cooled blunt body than for a slender uncooled body. However, reference 5 further postulates that stretching of vortex filaments near the nose of the body may be an important factor in causing flow instability. Even the theoretical guides are somewhat hazy at the present time.

Because of the absence of an understanding of the transition phenomenon on blunt bodies, a program was undertaken in a blowdown jet installed in the Langley gas dynamics laboratory at a Mach number of 4.95 and Reynolds number per foot of 73.2×10^6 to determine transition locations on 2-inch-diameter hemispheres for various wall-to-stream stagnation-temperature ratios. Initial values of the wall-to-stream stagnation-temperature ratios were 0.16 and 0.65. It was believed that such a program might supplement the existing results (summarized in ref. 2) which were obtained primarily in flight where Mach number, Reynolds number, and wall-to-stream stagnation temperature ratio all varied simultaneously. Furthermore, by performing the tests in a wind tunnel, the model could be examined before and after each test for possible roughness effects. The feasibility of using this particular jet for the transition investigation was established by the exceedingly large Reynolds numbers at which completely laminar flows were obtained on hemispheres in this jet. (See ref. 7.) Although the difficulties inherent in the flight measurements were eliminated in the present program, a different problem, the possibility of ice and carbon dioxide condensing on the model to form roughness, was introduced.

SYMBOLS

c_w	specific heat of model-skin material
D	diameter of hemisphere
h	heat-transfer coefficient
k	local thermal conductivity outside boundary layer
M	Mach number
N_{Nu}	Nusselt number, $\dfrac{hs}{k}$
N_{Pr}	Prandtl number
$N_{Re,D}$	free-stream Reynolds number based on model diameter, $\dfrac{\rho_\infty V_\infty D}{\mu_\infty}$
$N_{Re,s}$	local Reynolds number, $\dfrac{\rho u s}{\mu}$
$N_{Re,\epsilon}$	local Reynolds number based on roughness height, $\dfrac{\rho_\epsilon u_\epsilon \epsilon}{\mu_\epsilon}$
$p_{t,\infty}$	free-stream stagnation pressure
R	radius of hemisphere
s	distance along surface of model measured from stagnation point
T	temperature
T_r	recovery temperature
T_w	wall temperature
$T_{w,i}$	inside wall temperature of model skin
$T_{w,o}$	outside wall temperature of model skin
$T_{t,\infty}$	free-stream stagnation temperature

t   time

u   local velocity at outer edge of boundary layer

u_ϵ local velocity at top of roughness element

V_∞ free-stream velocity

ϵ roughness height

θ angular position from stagnation point, $\dfrac{57.3s}{R}$, deg

μ local viscosity at outer edge of boundary layer

μ_ϵ local viscosity at top of roughness element

μ_∞ free-stream viscosity

ρ local density at outer edge of boundary layer

ρ_w density of model-skin material

ρ_ϵ local density at top of roughness element

ρ_∞ free-stream density

τ skin thickness

APPARATUS, TESTS, AND METHODS

Jet

  The tests were performed in a 9-inch-diameter blowdown jet (closed test section) installed in the Langley gas dynamics laboratory. The circular nozzle was designed by the method of characteristics, and the ordinates were corrected for boundary-layer growth by assuming a turbulent boundary layer. The calibrated Mach number in the test section is approximately 4.95 with a maximum deviation of about 0.04 from this nominal value. The stagnation-pressure range of the jet when empty is 275 to 2,500 lb/sq in. with an atmospheric discharge. Stagnation pressures as low as approximately 50 lb/sq in. can be obtained by discharging into an existing vacuum system. The stagnation-temperature range of the

blowdown jet is from 0° F to $1,000^\circ$ F; however, the lower limit is set by condensation of oxygen in the nozzle. This occurrence imposes a lower limit of about 350° F at the higher pressures.

Models and Instrumentation

Models.- Three 0.060-inch-thick 2-inch-diameter hemispherical models, which were made as identical as practical to serve as a cross-check on the results, were used in this investigation. (See fig. 1.) The models were made of 17-4 PH stainless steel because, after being machined, it could be hardened without significant distortion. In this application the stainless steel was hardened to a Rockwell number of 40 in order to better resist particle abrasion in the airstream. The average thickness of any of the models varied less than 0.003 inch from the nominal 0.060-inch values. However, in all cases the skin-thickness variations around a given model were less than 0.001 inch. The models were polished as smooth as practical with a reasonable effort. A more detailed discussion of the model surface conditions is presented in the section entitled "Test Conditions." For convenience, the models are designated A, B, and C.

Instrumentation.- Ten iron-constantan thermocouples were spotwelded to the inner surface of each sphere at 10° spacings from the stagnation point. Extreme care was taken in the installation of each thermocouple to insure good contact and to eliminate any other lead from approaching a thermocouple junction and acting as a heat sink. The thermocouple outputs were recorded on an 18-channel galvanometer. The interior of the model was evacuated during the tests by means of a tube which was connected to a vacuum pump and inserted into the rear of the sting.

Installation

The models were sting supported from the rear on a side mounting plate as shown in figures 2 and 3. After uniform flow was established in the test section at the proper stagnation conditions, a vertical door was lowered. During the lowering process, air induced from the room choked the jet. When the vertical door was fully retracted (condition shown in fig. 3), it triggered the horizontal actuating cylinder which inserted the model into the test section in less than 0.1 second. Flow was reestablished almost immediately. In order to minimize any model pitting from particles in the airstream, the model was retracted from the tunnel within about 4 seconds after injection into the tunnel.

Two separate arrangements were used for inserting the model into the jet and the method depended upon the different initial wall temperatures. When the model was installed at room temperature, the procedure

just discussed and indicated in figures 2 and 3 was used. However, before the model in a cooled state (wall-to-stream stagnation-temperature ratio of 0.16) was injected into the jet, it was first installed on the sting support outside the jet. The model was then enclosed by wood blocks (split in half along a horizontal parting plane) as indicated in figure 4. A plan-form view is shown in figure 4(a) and a cutaway side view in figure 4(b). The wood blocks were held together in position around the model with small wood-dowel pins and with glue along the parting plane. In order to cool the model, the reservoir between the model and the wood blocks was flooded with liquid nitrogen through the fill hole at the top. The model was kept completely submerged in the liquid nitrogen bath outside the jet until the model temperature was uniform and at liquid nitrogen temperature. The entire assembly was then inserted into the jet which was at the proper test stagnation conditions. Immediately upon insertion into the jet, the blocks opened because of the forces on the beveled faces. The blocks opened by pivoting about the rear retainer collar which prevented them from sliding rearward and scratching the model. From high-speed motion pictures (about 2,000 frames/sec) and detailed examination of the models after each test, there was no evidence of model damage from the wood blocks.

Test Conditions

The approximate values of the free-stream test conditions were as follows:

Mach number 4.95
Angle of attack, deg 0
Stagnation temperature, $^\circ$F 400
Stagnation pressure, lb/sq in. abs 2,550
Reynolds number per foot . . . . 73.2×10^6
Reynolds number based on model diameter . . . . 12.2×10^6

The stagnation temperature, stagnation pressure, and free-stream Reynolds number varied slightly for each test; the specific values for each test are presented in table I.

Model wall temperature.- Two sets of initial model wall temperature were used: 100° F (room temperature) and -320° F (liquid nitrogen). Five tests were made with the three models. For one test, the model was initially at room temperature (referred to herein as a "hot test"); for four tests, the models were initially at -320° F (referred to herein as "cold tests"). The tests are designated 1A, 2A, 3B, 4B, and 5C. This system indicates that model A was used for the first two tests, model B for the next two tests, and model C for the last test. Test 1A was hot; the remaining tests were cold.

Model surface conditions.- An attempt (which was only partly successful) was made to establish quantitative limits on the surface finish of the three models. The models were examined with a 40-power microscope and with a CEJ Multimi 3000 multiple interference microscope. Interferograms were taken at seven positions on each model. Each interferogram covered only an area of approximately 1/16 inch square so that at best this procedure represented a very limited surface sampling. Based on this sampling, the surface finish of the three models was initially (that is, prior to tests 1A, 3B, and 5C) better than 2 to 3 microinches with some isolated depression scratches or depression pits about 10 to 20 microinches. It can only be conjectured that these finishes were representative of the entire models. Of the three models, model A had the poorest finish (poor only in a relative sense) and was used for the hot test. The best models, B and C, were reserved for the more critical cold tests.

Data Reduction

The heat-transfer data for the models were evaluated by means of the calorimeter technique. The heat entering the front face of the model was equated to the heat stored in the model by assuming that lateral conduction, the temperature difference across the skin thickness, and radiation are negligible for all times. For such a case, the heat balance for a thin hemispherical shell of constant thickness is, when the square of τ/R is neglected,

$$ h = \frac{\rho_w c_w \tau}{T_r - T_{w,i}} \frac{dT_{w,i}}{dt} \left(1 - \frac{\tau}{R}\right) \tag{1} $$

In the evaluation of h, as given by equation (1), the determination of the specific heat of the model material c_w at low temperatures presented quite a problem. Of course, since the primary purpose of the present program was to study transition location, the need for precisely evaluating the heat-transfer coefficient is of secondary importance. Transition locations could be established directly from visual observation of the galvanometer record of the thermocouple output since, in all cases, the temperature potential $\left(T_r - T_{w,o}\right)$ was large enough that a marked slope change in the temperature-time history accompanied the occurrence of transition. Nevertheless, for quantitative evaluation of the data, it is important to establish limits on the accuracy of the heat-transfer coefficients.

The model material, 17-4 PH stainless steel, was selected solely
for reasons of abrasion resistance; but, unfortunately, accurate meas-
urements of its specific heat are not available. For the hot test (1A),
the specific heat of 17-4 PH stainless steel was evaluated from a
weighted average of its constituents. In all cases the specific heat
was evaluated for a temperature corresponding to the average value of
the inside and outside wall temperatures. For the temperature range of
this test, this procedure should yield reasonably reliable values. For
the cold tests (2A, 3B, 4B, and 5C), the specific-heat values were
obtained from reference 8 and are presented in figure 5 with the values
for the hot test. The values in reference 8 were specified as stainless
steel, but the composition of the steel was not indicated. A comparison
of the two sets of specific heats at 100° F where the data overlap indi-
cates that the values used for the cold tests are low by as much as
10 percent. If the discrepancy were to carry through to low temperatures,
the indicated heat-transfer coefficients (eq. (1)) in the cold tests
would be too low by an amount proportional to the error in the specific
heat.

In order to establish further the limitations on the data imposed
by the assumptions made in obtaining equation (1), the effects of the
approximations will be considered. The net radiant-heat transfer between
the model and its surroundings was completely negligible because of the
relatively low wall temperatures. For the data obtained almost immedi-
ately after the model was inserted into the airstream, the lateral con-
duction effects were also negligible because the model temperature did
not differ significantly from the isothermal condition. However, for
the data obtained at later times (t ≈ 2 seconds), the lateral conduction
correction amounted to as much as 10 percent. This correction was not
applied because of its extremely approximate nature and because these
data obtained at the later time were used only for transition location.

The effect of normal conduction across the skin thickness because
of the finite skin conductivity was evaluated, and the data were cor-
rected in the following manner. The response of a thermocouple located
on the inner surface of the skin to a heating rate proportional to the
difference in recovery temperature and outer surface skin temperature
was computed from a solution of the one-dimensional, unsteady-heat-flow
equation. (See ref. 9.) From this calculation, the output of an inner-
surface thermocouple $\left(T_{w,i} \right)$ could be compared with the true heat-
transfer coefficient given as a boundary condition in the one-dimensional
calculation. This comparison established a correction factor that was
directly applicable to the data. This factor amounted to a maximum
increase of 11 percent in the heat-transfer coefficient as given by
equation (1) at a value of 0.166 for h. The correction is essentially
proportional to h. In addition, the outside-wall temperature was also
established in the process. Of course, these corrections are strictly

valid only when the assumed boundary condition on the heat-conduction
equation (that is, constant h) occurs. Realistically, this boundary
condition existed during a given test for all thermocouples for all
times until transition[1] occurred. It then ceased to exist for all
thermocouple locations at which the heat-transfer coefficient changed
because of transition.

No attempt was made to measure the recovery temperature because the
evaluation of the heat-transfer coefficient on blunt bodies does not
depend upon a precise measurement of the recovery temperature provided
the temperature potential $\left(T_r - T_{w,o}\right)$ is sufficiently large. Further-
more, if the models remained in the flow sufficiently long to establish
recovery temperatures, fine particles in the airstream would probably
strike the model surfaces and roughen them sufficiently to cause tran-
sition. This occurrence would invariably result in turbulent-flow
recovery temperatures. Hence, the calculated recovery temperatures were
used; these temperatures were based on either the square root or cube
root of the Prandtl number (by using local conditions outside the bound-
ary layer) with the choice depending upon whether the data were laminar
or turbulent. In all cases, the actual choice is indicated in table I.
Since, with the possible exception of the transition region, the proper
choice of laminar or turbulent recovery factor was quite apparent from
the data, errors introduced by this procedure would be negligible.

RESULTS AND DISCUSSION

Basic Data

The heat-transfer data for the hot test (initial wall temperature
approximately 100° F) are presented in figure 6, and the data for the
cold tests (initial wall temperature approximately -320° F) are presented
in figures 7 to 9. For each test, the wall-temperature distribution
$T_{w,o}$, the heat-transfer coefficient h, and the laminar correlating

parameter $\dfrac{N_{Nu}}{\sqrt{N_{Re,s}}}$ are presented for representative times. Since the

results of reference 7 previously established that it was possible to
obtain completely laminar flows for the hot-test condition, only one
test was made to verify these results. Four cold tests (figs. 7 to 9)

---

[1]The term "transition" in the present paper is used in a general
sense and also includes changes from turbulent to laminar flow.

were made at essentially the same stagnation conditions to evaluate the reproducibility of the transition occurrence.

Hot test, 1A.- The heat-transfer results for the hot test (1A) agree in all essential details with the findings of reference 7. The boundary layer on the hemisphere is initially completely laminar (fig. 6) as evidenced by the excellent agreement between the data obtained during the early part of the test and the curve for the laminar theory of reference 10. There is, perhaps, some evidence of transition rearward on the hemisphere for t = 0.9 second. If, however, transition has occurred for this condition, the change in heat-transfer level due to transition is still relatively small. For t = 1.1 seconds, transition occurs rearward of the 30° station and the flow clearly becomes turbulent. Transition to turbulent flow resulted from surface roughness caused by the impact on the model surface of small particles in the airstream. The roughness present at the conclusion of test 1A was quite extensive and too large to measure with the multiple interference microscope. This microscope could resolve random roughness of the order of 50 microinches without too much difficulty. With the aid of the 40-power microscope, it was determined that pit diameters in excess of 0.005 inch were common. As will be demonstrated subsequently, if the roughness height associated with the pits is only one-tenth of the pit diameter (that is, a roughness height of 500 microinches), roughness-induced transition will occur.

The turbulent estimate (made by M. Richard Dennison while employed by the Missile Systems Division of Lockheed Aircraft Corporation and presented in a paper not generally available) for the data obtained at a later time of 1.1 seconds is quite inadequate. However, as pointed out in reference 7, the ability of the turbulent estimate for predicting experimental results is related to the transition location. The agreement between the present data and the turbulent estimate would be significantly improved if transition were to occur more forward since it is assumed in the theory that the flow is completely turbulent right from the stagnation point.

Cold tests, 2A, 3B, 4B, and 5C.- The heat-transfer results for the cold tests, particularly those in figure 9, are in marked contrast to the hot-test results shown in figure 6. In each cold test, unlike in the hot test, the boundary layer was initially turbulent over a major portion of the hemisphere. For two of these tests, 3B and 5C, the boundary layer was at later times[2] (that is, at t = 2.0 seconds and t = 1.2 seconds, respectively) almost completely laminar as judged by

---

[2]It is of importance to note that surface abrasion due to particle impacts was significantly less severe during the cold tests than during the hot test. Hence, the cold-test data obtained at later times are not as badly plagued by roughness effects.

a comparison of these data with laminar theory. (See ref. 10.) This reverse transition with time (or realistically with increasing wall temperature) from turbulent to laminar flow was much more clearly evident in the galvanometer records of the temperature-time histories. A typical record (test 5C) is shown in figure 10. In this record, the individual curves are the outputs of thermocouples located at the angular positions indicated. The timing lines are 0.1 second apart. An approximate scale has been shown for conversion of galvanometer displacement to temperature difference. Transition from a turbulent boundary layer to a laminar boundary layer can be inferred from the large curvature of the galvanometer records of the rearward thermocouples between 0.7 and 1.1 seconds (transition region in fig. 10) after the start of the test. Although the change in slope (and hence heat transfer) is quite pronounced, the time interval over which it takes place is several tenths of a second. This long time interval is in marked contrast to the galvanometer record (fig. 11) for the hot test in which transition from laminar to turbulent flow occurred practically with a slope discontinuity. This "sharpness" of transition is characteristic of all records (the present investigation and those of ref. 7) obtained on the hemisphere in which roughness caused transition. It is to be noted that the relatively long transition time for the cold test is much longer than the time required for the effects of a change in heating to diffuse through the skin and hence not an effect of conductivity of the skin. This effective diffusion time of the skin must be 0.1 second or less, as can be judged from the initial portion of the temperature-time histories (figs. 10 and 11) when the model is inserted into the airstream. It is therefore postulated that the much smoother change in slope in the galvanometer record associated with transition from turbulent to laminar flow (as contrasted to the sharp break associated with transition from laminar to turbulent flow caused by roughness) may indicate that the initially turbulent boundary layer in the cold tests is of nonroughness origin. The possibility of ice or solid carbon dioxide forming roughness on the model and hence causing turbulent flow at the low wall temperatures is considered in detail subsequently. The results (figs. 6 and 9) appear to substantiate the contentions (ref. 2, for example) that sufficient cooling is destabilizing on hemispherical bodies. Quantitatively, the results are not contrary to the correlation of reference 2.

No data obtained at later times during the tests have been presented for tests 2A and 4B because the flow remained turbulent for all times subsequent to those times shown. The fact that no transition back to laminar flow occurred with increasing wall temperature for these two tests is attributed to roughness on the model surface which occurred in a previous test. In both cases, a previous test was made on the same model. Furthermore, the model was polished between tests 1A and 2A but not between tests 3B and 4B. It is known that model A was roughened sufficiently during test 1A to cause transition (fig. 6). Apparently the polishing was inadequate to remove all the critical roughness for

test 2A. A detailed examination of the model after test 2A indicated significantly less additional impact pits than occurred in test 1A. Nevertheless, the magnitude of some of the pits was as large as 0.005 inch in diameter - the magnitude which was present after test 1A. Here again, if the roughness height is only one-tenth of the pit diameter, roughness-induced transition will occur as is discussed subsequently.

Test 4B was the second test on model B (test 3B was the first). It is very likely that model B was roughened sufficiently after t = 2.0 seconds during test 3B to cause transition at later times in test 3B and permanent transition for test 4B. An examination of the model after test 4B indicated essentially the same status as was noted after test 2A. It must be concluded, therefore, that the occurrence of turbulent flow during test 2A and 4B is of roughness origin and should be discarded from any discussion of nonroughness-induced transition due to cooling. In fact, if the original test program calling for only one test per model had been followed, tests 2A and 4B would not have existed, and this apparently extraneous difficulty would not have occurred.

A comparison of the laminar data obtained at later times of tests 3B and 5C with laminar theory indicates (fig. 9) discrepancies that are considerable, particularly when the excellent correlation obtained for the hot test is considered (fig. 6). Based on the more exact theoretical stagnation-point heat-transfer calculations of reference 11, the influence of large cooling has a negligible effect on

the stagnation value of $\dfrac{N_{Nu}}{\sqrt{N_{Re,s}}}$ for the range of parameters of the

present investigation. The main cause of the discrepancy is the uncertainty in the model specific heat. For example, the temperature variations from t = 0.2 second to t = 1.4 seconds during test 3B were sufficient to cause the specific heat to change by a factor of 2 according to the estimate presented in figure 5. In fact at t = 2.0 seconds, there is sufficient temperature variation around the model to cause a 15-percent variation in specific heat. Hence, errors introduced by the uncertainty in the specific-heat level and variation with temperature are of sufficient magnitude to account for a significant part of the discrepancies. It is of interest to note that the excellent prediction of the stagnation-point data for the hot test may be interpreted to indicate that the stagnation-point heating-rate measurement together with theory may be a very convenient method for determining, approximately, the specific heats of materials over a reasonably wide temperature range.

Evaluation of Possible Roughness Effects

on Transition During Tests

On the basis of the results presented in figures 6 to 11, it appears that lowering the wall temperature below a certain value is destabilizing - the destabilization resulting in a nonroughness-induced transition to turbulent flow on the hemispheres. This idea has been postulated before (ref. 2, for example), and each time the suggestion of such a phenomenon has been sufficient to initiate discussion pro and con. The primary objection is usually an intuitive one - such an occurrence is contrary to the cooling effect in the classical flat-plate stability theory. Furthermore, there is no satisfying theoretical basis to prove that such a phenomenon should occur on blunt bodies. In each experimental case a plausible argument can be advanced that roughness effects, rather than a new transition phenomenon, cause the observed occurrences. This argument is a reasonable one in that as the wall temperature decreases, the boundary layer thins and a particle of fixed roughness height becomes more significant in causing transition. Because of the paramount importance of roughness in the discussion, some detailed calculations have been made to establish the magnitude of roughness required to cause transition and to determine, if possible, whether roughness could be a dominant effect in the present test. These results are presented with the full realization that they are far from conclusive; yet they indicate that roughness does not appear to be a dominant factor in causing transition from turbulent flow to laminar flow as the body is warmed during tests 3B and 5C.

Roughness Reynolds number criterion.- Recent work at subsonic (ref. 12) and at supersonic (ref. 13) speeds has established a criterion for transition caused by three-dimensional roughness particles. This criterion states that transition will be caused by roughness if the roughness Reynolds number, based on fluid properties at the top of the roughness element and the height of the roughness element, exceeds a specified value. Values of roughness Reynolds number as low as approximately 200 were adequate (ref. 13) to cause transition at supersonic speeds, though an average number between 400 and 600 might be more representative of the results of references 12 and 13. Furthermore, moderate cooling had little effect on this criterion. (See ref. 13.) If it is assumed that the roughness Reynolds number concept can be extrapolated to the conditions of the present investigation, that is, for bodies of high curvature and extreme cooling, then an estimate of the roughness Reynolds numbers for the hemisphere for the present test conditions might yield an insight into the magnitude of roughness required to cause transition.

Calculations of the roughness Reynolds number, made according to the procedures of reference 14, are presented in figure 12 as a function

of angular position for the free-stream conditions of the present investigation and for wall temperatures of -288° F and 56° F. These wall temperatures correspond to wall-to-stream stagnation-temperature ratios of 0.2 and 0.6, respectively. In making these calculations, the fluid properties were assumed to vary linearly from the wall values to the values at the top of the roughness element. This approximation is reasonable because in the region of transition (tests 3B and 5C) the maximum roughness height of 100 microinches assumed in the calculation is small in comparison with the boundary-layer thickness.

Transition occurred at the following approximate locations and wall temperatures (figs. 6 to 9)

Test	θ, deg	$T_{w,o}$, $^\circ$F
1A (hot)	35	180
3B (cold)	35	75
5C (cold)	25	-60

Therefore, from figure 12, it can be established that a particle roughness size of the order of 100 microinches (120 microinches for test 1A; 105 microinches for test 3B; and 85 microinches for test 5C as determined from additional calculations) would be required to cause transition for either the hot or cold tests if a conservatively low transition roughness Reynolds number of 100 is assumed. For the hot test, roughness of this size would require a particle impact during the test since the flow was laminar for the earlier part of the test, and the surface finish was certainly far superior to 120 microinches initially. As pointed out previously, examination of model A after test 1A clearly established pitting of sufficient magnitude to cause transition. For the cold tests the flow was initially turbulent and then became laminar. For this phenomenon to occur the roughness, if indeed it were roughness, must disappear or become less significant during the test. Such would be the case if the roughness were caused by ice or solid carbon dioxide formation on the model surface,[3] or if the boundary layer thickened sufficiently to eliminate roughness effects as the model heated. The ice

---

[3]Though there is approximately 1-percent argon in atmospheric air, the effects of argon condensation are completely negligible because of argon's low boiling point (approximately -303° F) and low heat of sublimation (approximately 80 btu/lb).

sources are water vapor remaining in the air of the jet after drying
and water vapor in the reservoir at the time the liquid nitrogen was
introduced into the reservoir. The source of carbon dioxide is atmos-
pheric air (3 parts of carbon dioxide per 10,000 parts of air) which is
used in the jet. These effects are considered in the next sections.

Condensation effects - jet conditions.- In order to study condensa-
tion effects in the jet, a water phase diagram for vapor and solid is pre-
sented in figure 13, and a phase diagram for carbon dioxide is presented
in figure 14. In these figures, the solid state is to the left of the
boundary line and the vapor state is to the right of the boundary line.
Superposed on these diagrams are two curves. One curve corresponds to
isentropic flow in the jet and the second curve corresponds to isentropic
flow around the model (based on local conditions outside the boundary
layer). For the water phase diagram, these two curves were computed for
a homogeneous vapor mixture (even in the solid domain) corresponding to
a weight ratio of water to air of 10^{-6} or a dewpoint of about -16° F at
5,000 lb/sq in. Inasmuch as the air for the present tests was dried at
5,000 lb/sq in., it is known that the specific humidity is very low,
between 10^{-6} and 10^{-9}. The actual value depended upon the state of the
driers at the time of the tests and was closer to 10^{-6}. To be conserva-
tive, that is to maximize the water content, the value 10^{-6} has been used.
For the carbon dioxide phase diagram, the normal atmospheric weight ratio
of carbon dioxide to air of 3×10^{-4} was assumed. From these diagrams
(figs. 13 and 14), it is clear that for both cases condensation in the
nozzle occurs downstream of the Mach number 2 location. Furthermore,
if the mixtures (figs. 13 and 14) are in equilibrium, then the local
flow around the model is always in the vapor state. Consequently, the
only way an icing problem can occur is when the vapor enters the bound-
ary layer and contacts the model surface. This point is considered in
the next section. If the flow is out of equilibrium, that is the solid
formed in the nozzle does not vaporize immediately on passing through
the model bow shock, the solid particles will bounce off the model sur-
face. Since the flow eventually becomes laminar (tests 3B and 5C), any
such particles striking the model are of no consequence in causing model
roughness.

Condensation effects - model boundary-layer conditions.- For the
cold tests, water vapor or carbon dioxide entering the boundary layer
may condense on the model surface (which acts as a cold trap) provided
the surface temperature is less than approximately -70° F for water
vapor and less than approximately -200° F for carbon dioxide. (No con-
densation is possible during the hot test.) In order to establish an
order of magnitude of the maximum amount of roughness which would result
from condensation of all the vapor (water or carbon dioxide) in the

boundary layer, an estimate of the boundary-layer thickness (as defined by a 0.5-percent velocity decrement) was made at the 90° station by using the procedure of reference 14. This boundary-layer thickness, together with the displacement thickness and local velocity outside the boundary layer, established the maximum amount of vapor available for condensation. If, for convenience, it is assumed that all the vapor were to condense uniformly over the hemisphere, then the ice covering the model would grow with an initial rate of 0.16 microinch per second and the carbon dioxide would grow with an initial rate of 29.1 microinches per second. Clearly, the magnitude of ice condensing in 1 second (time to exceed -70° F by a considerable margin) would be inadequate to cause roughness transition. For carbon dioxide the time to exceed -200° F in the vicinity of transition is about 0.3 second so that a layer of solid carbon dioxide of the order of 9 microinches might be possible. It would take, therefore, a local rate of growth at least an order of magnitude larger than this estimated growth to produce enough solid carbon dioxide roughness to cause transition. Such an occurrence is unlikely.

Condensation effects - reservoir conditions.- One additional source of water vapor for ice condensation on the model is the air that is present in the reservoir (fig. 4(b)) at the time of liquid nitrogen filling. Of course, in the filling process every effort was made to flood the reservoir so as to submerge instantly the complete model. Submerging the model was usually accomplished in less than a second. Once the model was submerged in the liquid nitrogen it stayed submerged until the wood reservoir blocks were blown apart during the test. Although the reservoir volume was small, approximately 7 cubic inches, all the moisture in this air, if condensed on the hemisphere, would form a uniform layer of ice about 14 microinches thick.[4] Since the surface area of the reservoir was much larger than that of the model, and the liquid nitrogen acted as a cold trap, a more realistic estimate of the maximum possible ice thickness would be 5 microinches or less. The model was visually examined through the liquid nitrogen bath before insertion into the tunnel, and the surface appeared shiny with no apparent frost on the model. Of course, 5 microinches correspond to about 1,270 angstrom units - a fraction of a wavelength of visible light - and without a knowledge of the light absorption coefficient of the ice, it cannot be ascertained whether a coating of ice this thin would be visible to the eye. In any case, a thickness of 5 microinches or, for that matter, even 14 microinches would be inadequate to cause roughness transition for the earlier part of the tests and low wall temperatures. Unfortunately, the model could not be examined during the test because of the absence of windows in the tunnel.

---

[4]For this estimate, any water vapor pumped out during the filling process is neglected. Furthermore, any carbon dioxide condensation in the reservoir can be neglected because the quantity is insignificant in comparison with the quantity of carbon dioxide condensed from the boundary layer and with the water vapor in the reservoir.

Assessment of cold-test transition results.- As a final assessment
of the cold-test transition results, phase diagrams for tests 3B and 5C
are presented in figures 15 and 16 for a weight ratio of 10^{-6} for water
vapor and a weight ratio of 3×10^{-4} for carbon dioxide. Again, homoge-
neous mixtures in equilibrium are considered in establishing the local
vapor pressures for the experimental data. The experimental data are
presented as a function of wall temperature $T_{w,o}$. The dashed line
represents a transition time boundary established from the data. The
region enclosed by the boundary (to the lower left) represents a tur-
bulent regime whereas the region outside the boundary represents a
laminar regime. During both tests, transition back to laminar flow
takes place in the vapor phase region. If ice or solid carbon dioxide
on the model were the cause of the initial turbulent flow, then the
change to laminar flow would occur as the phase boundary is crossed.
The time delay in switching to laminar flow is, however, several orders
of magnitude longer than the time required to melt any reasonable amount
of ice or solid carbon dioxide formation. If a layer of ice of 15 micro-
inches or a layer of solid carbon dioxide of 29.1 microinches (conserva-
tive estimates for maximum amounts formed in 1 second) is assumed, the
melting time would be of the order of 0.002 second. Hence, condensation
effects should not be the cause of the initially turbulent flow. (No
attempt should be made to cross-plot these data to isothermal wall
conditions because transition at one location affects all rearward
locations.)

The occurrence of the initially turbulent flow might, on the other
hand, be attributed to slight model imperfections which become less
significant as the boundary layer thickens because of increasing wall
temperature. The probability of this happening is remote because there
are only minor changes in boundary-layer thickness for a laminar bound-
ary layer in the wall-temperature range of transition during the present
investigation. Also, the roughness sizes would still have to be of the
order of 100 microinches. Undoubtedly, roughness has a secondary influ-
ence on specific details of the flow changeover, but it must be concluded
that roughness is not the dominant factor in causing turbulent flow for
the early parts of tests 3B and 5C (low wall temperatures).

CONCLUDING REMARKS

Measurements of the location of boundary-layer transition and the
local heat transfer have been made on 2-inch-diameter hemispheres in the
Langley gas dynamics laboratory at a Mach number of 4.95, a Reynolds
number per foot of 73.2×10^6, and a stagnation temperature of approxi-
mately 400° F. The transient-heating thin-skin calorimeter technique

18

was used, and the initial values of the wall-to-stream stagnation temperature ratios were 0.16 (cold tests) and 0.65 (hot test).

During two of the four cold tests, the boundary-layer flow changed from turbulent to laminar over large regions of the hemisphere as the model heated. On the basis of a detailed consideration of the magnitude of roughness possibly present during these two cold tests, it appears that this destabilizing effect of low wall temperatures (cooling) was not caused by roughness as a dominant influence. This idea of a decrease in boundary-layer stability with cooling has been previously suggested. (See, for example, NASA Memorandum 10-8-58E.) For the laminar data obtained during the early part of the hot test, the correlation of the local-heating data with laminar theory was excellent.

Langley Research Center,
    National Aeronautics and Space Administration,
        Langley Field, Va., March 3, 1960.

REFERENCES

1. Lees, Lester: The Stability of the Laminar Boundary Layer in a Compressible Fluid. NACA Rep. 876, 1947. (Supersedes NACA TN 1360.)

2. Wisniewski, Richard J.: Note on a Correlation of Boundary-Layer Transition Results on Highly Cooled Blunt Bodies. NASA MEMO 10-8-58E, 1958. (Supersedes NACA RM E57J14.)

3. Krasnican, M. J., and Rabb, L.: Effects of Nose Radius and Extreme Cooling on Boundary-Layer Transition for Three Smooth 15°-Cone-Cylinders in Free Flight at Mach Numbers to 8.50. NASA MEMO 3-4-59E, 1959.

4. Lees, Lester: Note on the Stabilizing Effect of Centrifugal Forces on the Laminar Boundary Layer Over Convex Surfaces. Jour. Aero. Sci. (Reader's Forum), vol. 25, no. 6, June 1958, pp. 407-408.

5. Kuethe, A. M.: On the Stability of Flow in the Boundary Layer Near the Nose of a Blunt Body. U.S. Air Force Project RAND Res. Memo. RM-1972 (ASTIA Doc. No. AD 150687), The RAND Corp., Aug. 28, 1957.

6. Ferri, Antonio, and Vaglio-Laurin, Roberto: A Note on the Effect of Centrifugal Forces and Accelerated Motion on the Instability of the Laminar Boundary Layer About Highly Cooled Bodies. PIBAL Rep. No. 313 (Contract No. AF 18(600)-693), Polytechnic Inst. Brooklyn, Dec. 1956. (Available From ASTIA as Doc. No. AD-115-002.)

7. Cooper, Morton, and Mayo, Edward E.: Measurements of Local Heat Transfer and Pressure on Six 2-Inch-Diameter Blunt Bodies at a Mach Number of 4.95 and at Reynolds Numbers Per Foot up to 81×10^6. NASA MEMO 1-3-59L, 1959.

8. Chelton, Dudley B., and Mann, Douglas B.: Cryogenic Data Book. UCRL-3421 (Contract No. W-7405-eng-48), Univ. of California, May 15, 1956.

9. Carslaw, H. S., and Jaeger, J. C.: Conduction of Heat in Solids. The Clarendon Press (Oxford), 1947, pp. 258-259.

10. Stine, Howard A., and Wanlass, Kent: Theoretical and Experimental Investigation of Aerodynamic-Heating and Isothermal Heat-Transfer Parameters on a Hemispherical Nose With Laminar Boundary Layer at Supersonic Mach Numbers. NACA TN 3344, 1954.

11. Beckwith, Ivan E.: Similar Solutions for the Compressible Boundary Layer on a Yawed Cylinder With Transpiration Cooling. NACA TN 4345, 1958.

L
7
5
2

12. Von Doenhoff, Albert E., and Horton, Elmer A.: A Low-Speed Experimental Investigation of the Effect of a Sandpaper Type of Roughness on Boundary-Layer Transition. NACA Rep. 1349, 1958. (Supersedes NACA TN 3858.)

13. Braslow, Albert L., Knox, Eugene C., and Horton, Elmer A.: Effect of Distributed Three-Dimensional Roughness and Surface Cooling on Boundary-Layer Transition and Lateral Spread of Turbulence at Supersonic Speeds. NASA TN D-53, 1959. (Supersedes NACA RM L58A17.)

14. Cohen, Clarence B., and Reshotko, Eli: The Compressible Laminar Boundary Layer With Heat Transfer and Arbitrary Pressure Gradient. NACA Rep. 1294, 1956. (Supersedes NACA TN 3326.)

L-752

TABLE I

EXPERIMENTAL HEAT-TRANSFER RESULTS[a]

Values of h, Btu/(sq ft)(sec)(°F), $T_{w,t}$, °F, and $T_{w,o}$, °F

Test 1A — $P_{t,\infty}$ = 2,545 lb/sq in.; $T_{t,\infty}$ = 406° F; $N_{Re,D}$ = 12.2 × 10^6

θ, deg	t = 0.2 sec			t = 0.9 sec			t = 1.1 sec		
	h	$T_{w,t}$	$T_{w,o}$	h	$T_{w,t}$	$T_{w,o}$	h	$T_{w,t}$	$T_{w,o}$
0	b0.1065	112	137	b0.1094	179	199	b0.1030	194	212
10	b.1066	112	137	b.1102	177	197	b.1046	192	210
20	b.0981	115	156	b.0977	170	188	b.0967	184	201
30	b.0851	112	152	b.0881	165	182	b.0889	176	192
40	b.0702	108	125	b.0744	153	168	.1114	170	184
50	b.0510	106	118	b.0603	141	155	.1133	154	165
60	b.0458	105	114	b.0550	132	142	.0969	144	154
70	b.0340	100	109	b.0458	125	131	.0776	133	141
80	b.0234	98	105	b.0303	114	120	.0609	122	128
90	b.0166	98	103	b.0220	108	112	.0445	114	119

Test 2A — $P_{t,\infty}$ = 2,555 lb/sq in.; $T_{t,\infty}$ = 407° F; $N_{Re,D}$ = 12.2 × 10^6

θ, deg	t = 0.2 sec			t = 0.5 sec		
	h	$T_{w,t}$	$T_{w,o}$	h	$T_{w,t}$	$T_{w,o}$
0	b0.0832	268	226	b0.0854	178	138
10	b.0784	269	228	b.0785	182	144
20	b.0773	267	227	b.0764	183	145
30	b.0727	267	230	b.0740	188	151
40	.0783	264	223	.0832	178	139
50	.1117	254	199	.0981	158	108
60	.1174	255	198	.1080	155	101
70	.0687	270	220	.0945	169	123
80	.0668	283	248	.0700	202	169
90	.0465	300	274	.0498	252	208

Test 3B — $P_{t,\infty}$ = 2,545 lb/sq in.; $T_{t,\infty}$ = 405° F; $N_{Re,D}$ = 12.0 × 10^6

θ, deg	t = 0.2 sec			t = 1.4 sec			t = 2.0 sec		
	h	$T_{w,t}$	$T_{w,o}$	h	$T_{w,t}$	$T_{w,o}$	h	$T_{w,t}$	$T_{w,o}$
0	b0.0802	260	218	b0.0776	-10	22	b0.0833	61	88
10	b.0754	260	220	b.0775	-13	17	b.0786	63	90
20	b.0752	260	220	b.0785	-12	18	b.0771	60	86
30	b.0847	251	207	b.0771	6	39	b.0702	70	98
40	.1119	257	180	.0870	24	62	.0654	89	118
50	.1158	232	173	.0870	38	77	.0599	93	124
60	.1089	240	185	.0801	16	54	.0520	71	101
70	.0870	259	215	.0752	-14	19	.0440	38	66
80	.0569	279	248	.0569	-75	-50	.0321	-28	-6
90	.0583	282	259	.0591	-123	-104	.0253	-84	-66

Test 4B — $P_{t,\infty}$ = 2,555 lb/sq in.; $T_{t,\infty}$ = 407° F; $N_{Re,D}$ = 12.2 × 10^6

θ, deg	t = 0.2 sec		
	h	$T_{w,t}$	$T_{w,o}$
0	b0.0782	258	217
10	b.0848	270	226
20	b.0857	256	211
30	.1036	237	176
40	.1512	218	145
50	.1628	210	128
60	.1334	228	161
70	.1024	245	192
80	.0657	272	237
90	.0574	296	274

Test 5C — $P_{t,\infty}$ = 2,555 lb/sq in.; $T_{t,\infty}$ = 419° F; $N_{Re,D}$ = 11.9 × 10^6

θ, deg	t = 0.2 sec			t = 0.6 sec			t = 1.2 sec		
	h	$T_{w,t}$	$T_{w,o}$	h	$T_{w,t}$	$T_{w,o}$	h	$T_{w,t}$	$T_{w,o}$
0	b0.0810	264	222	b0.0949	148	110	b0.0798	57	-4
10	b.0732	265	226	b.0787	157	121	b.0781	53	-22
20	b.0727	261	223	b.0800	156	121	b.0797	54	-23
30	.1040	247	194	.0942	133	86	.0744	54	-4
40	.1079	242	187	.1108	115	66	.0720	15	25
50	.1262	231	168	.1231	99	44	.0625	10	34
60	.1229	237	175	.1216	106	53	.0463	23	20
70	.0947	258	210	.1010	139	99	.0593	58	-22
80	.0567	283	252	.0651	191	162	.0376	114	-88
90	.0358	302	281	.0585	232	212	.0265	167	-148

[a]All values based on turbulent recovery factor unless otherwise specified.
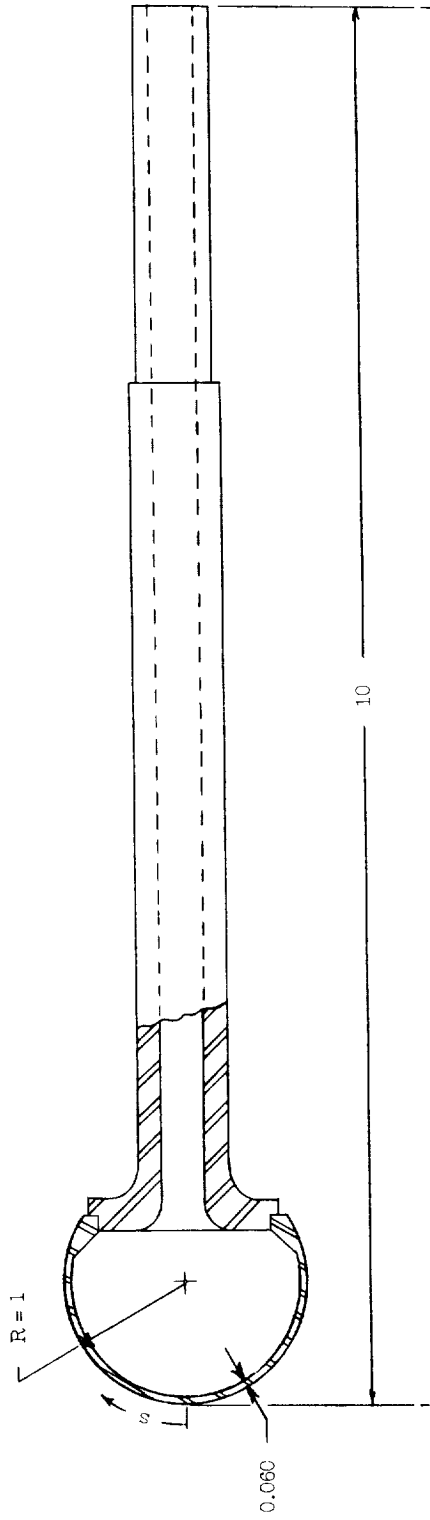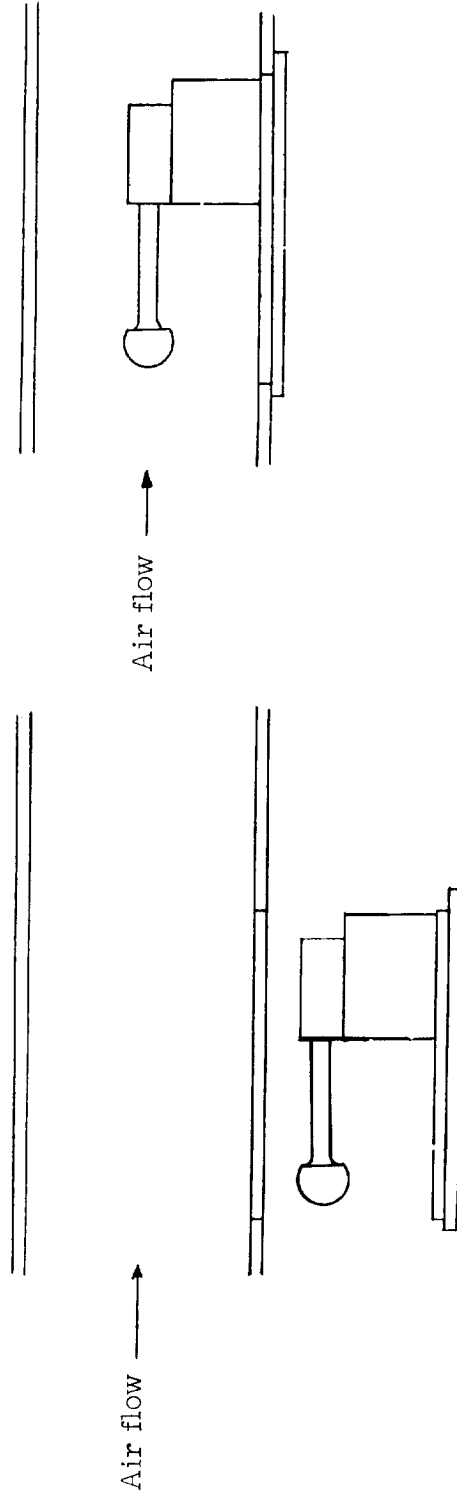[b]Values based on laminar recovery factor.

Figure 1.- Model geometry. All dimensions are in inches.

L-752

Air flow →

Air flow →

Model location prior to test

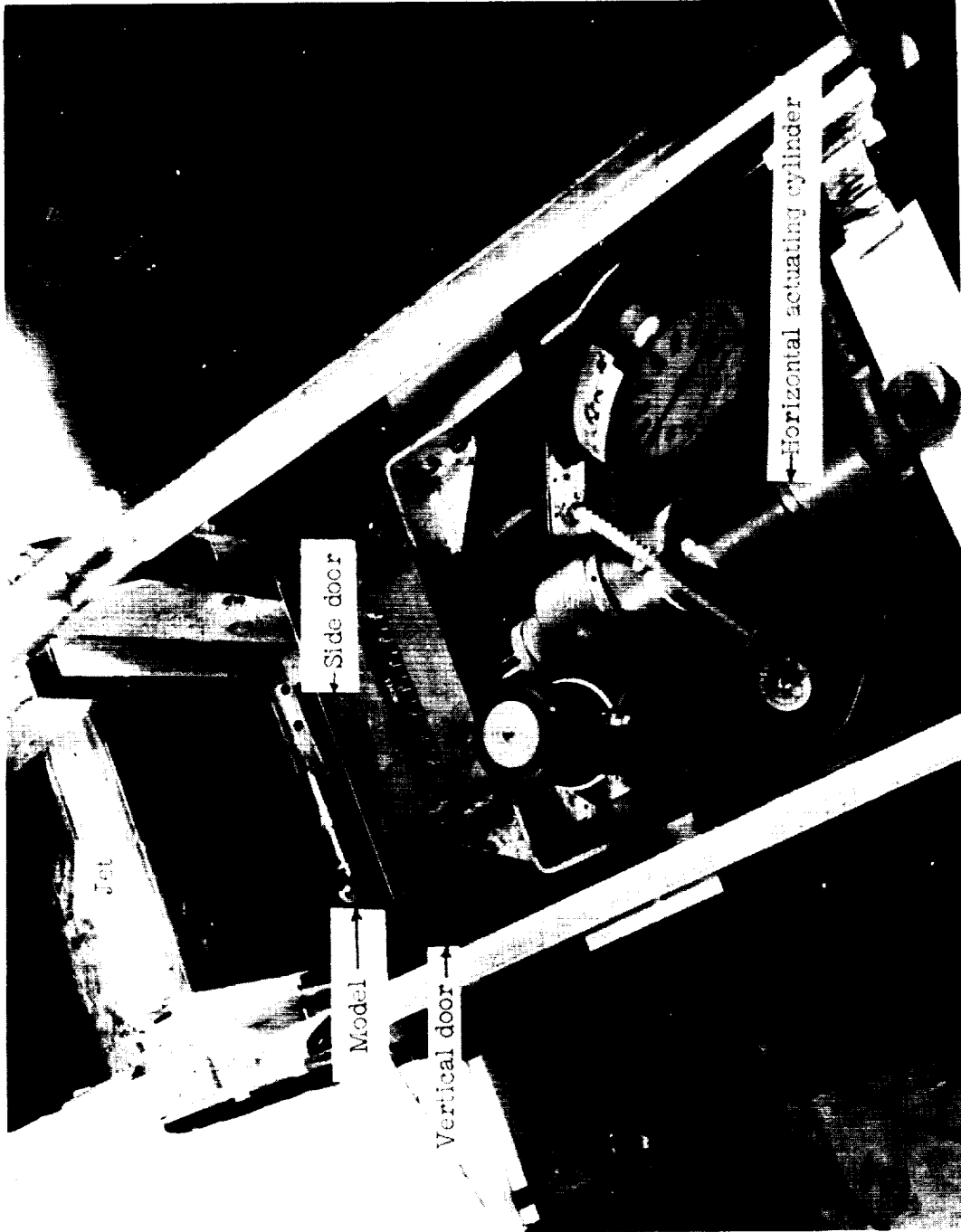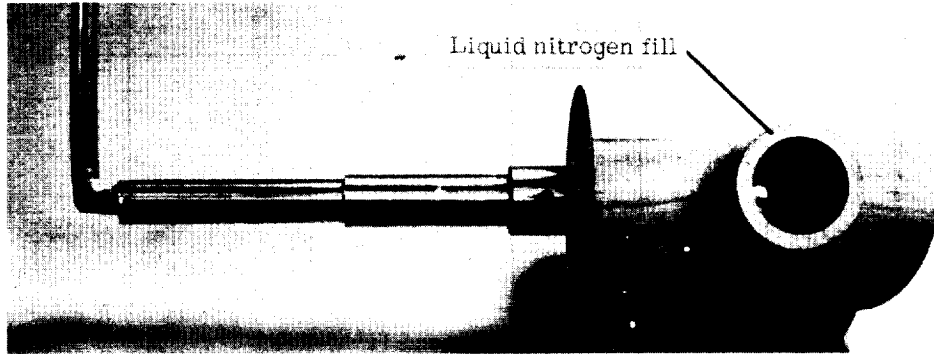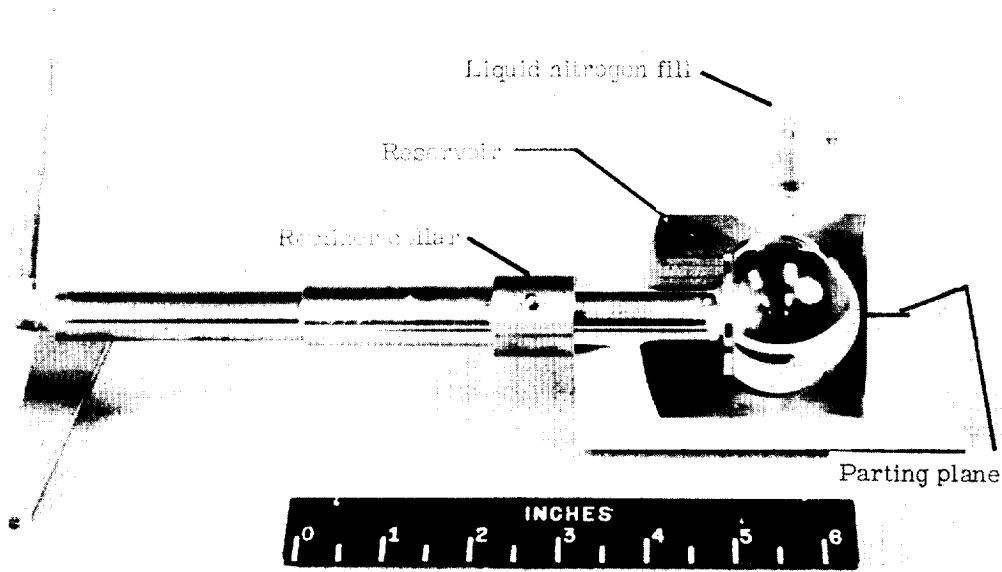Model location during test

Figure 2.- Side-support installation.

Figure 3.- Photograph of test installation. L-59-1481.1

(a) Model in cover.

(b) Cutaway side view of model in cover.   L-59-1950.1
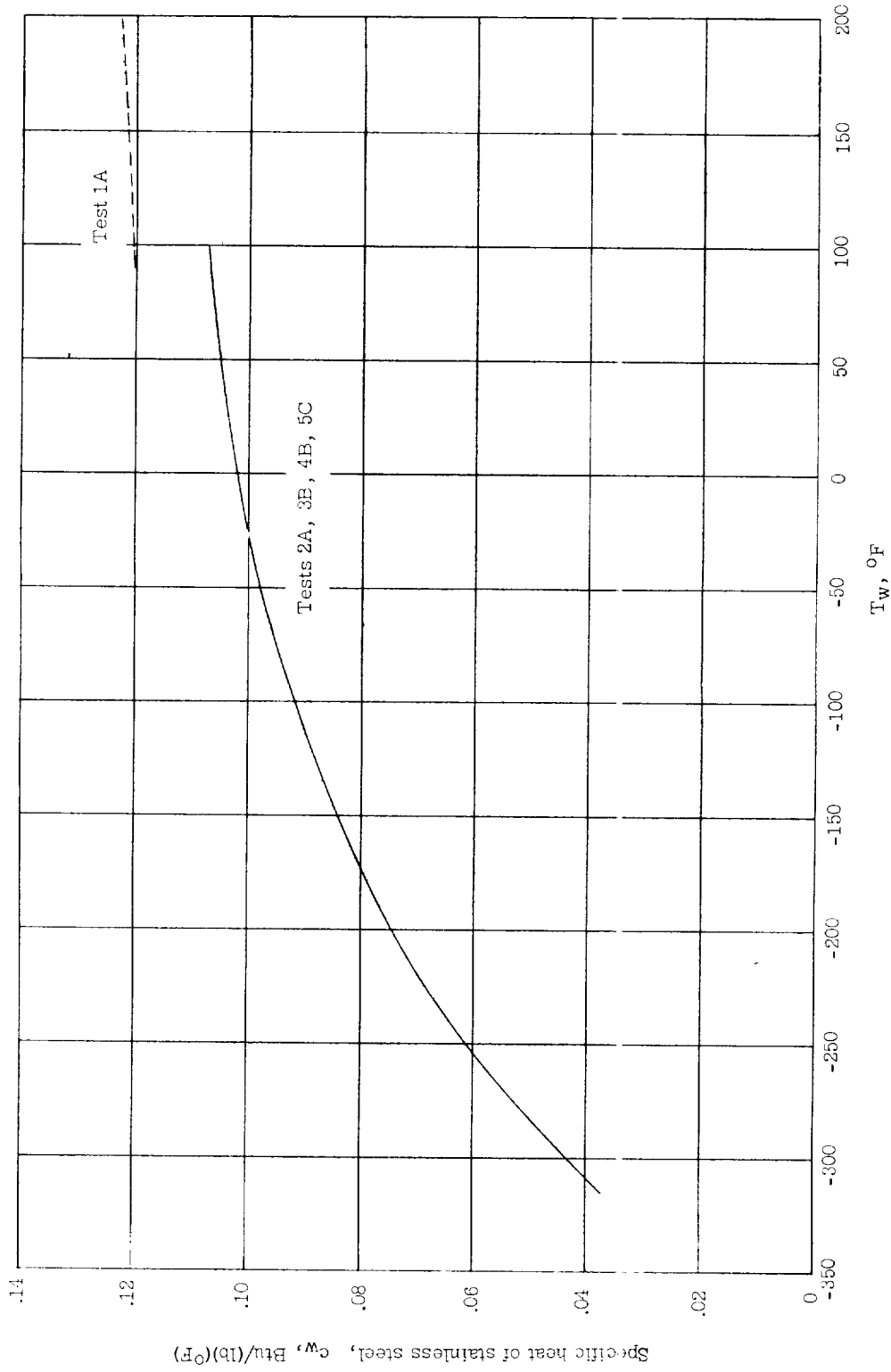
Figure 4.- Model and cover arrangement.

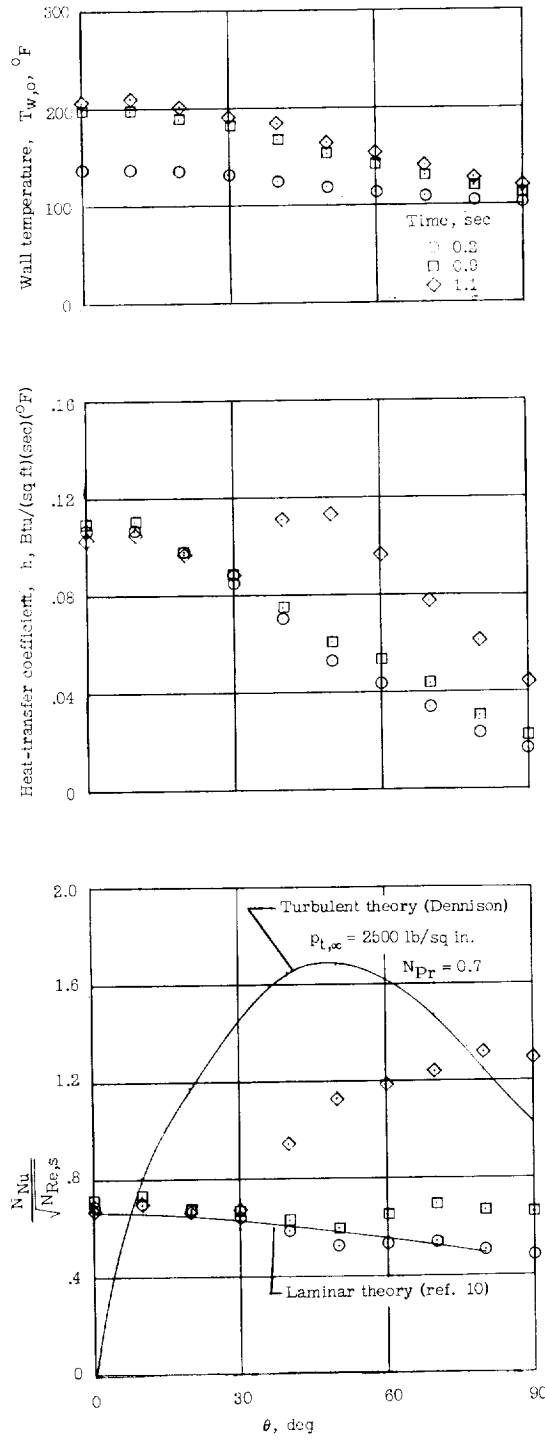Figure 5.- Specific-heat variation with wall temperature.
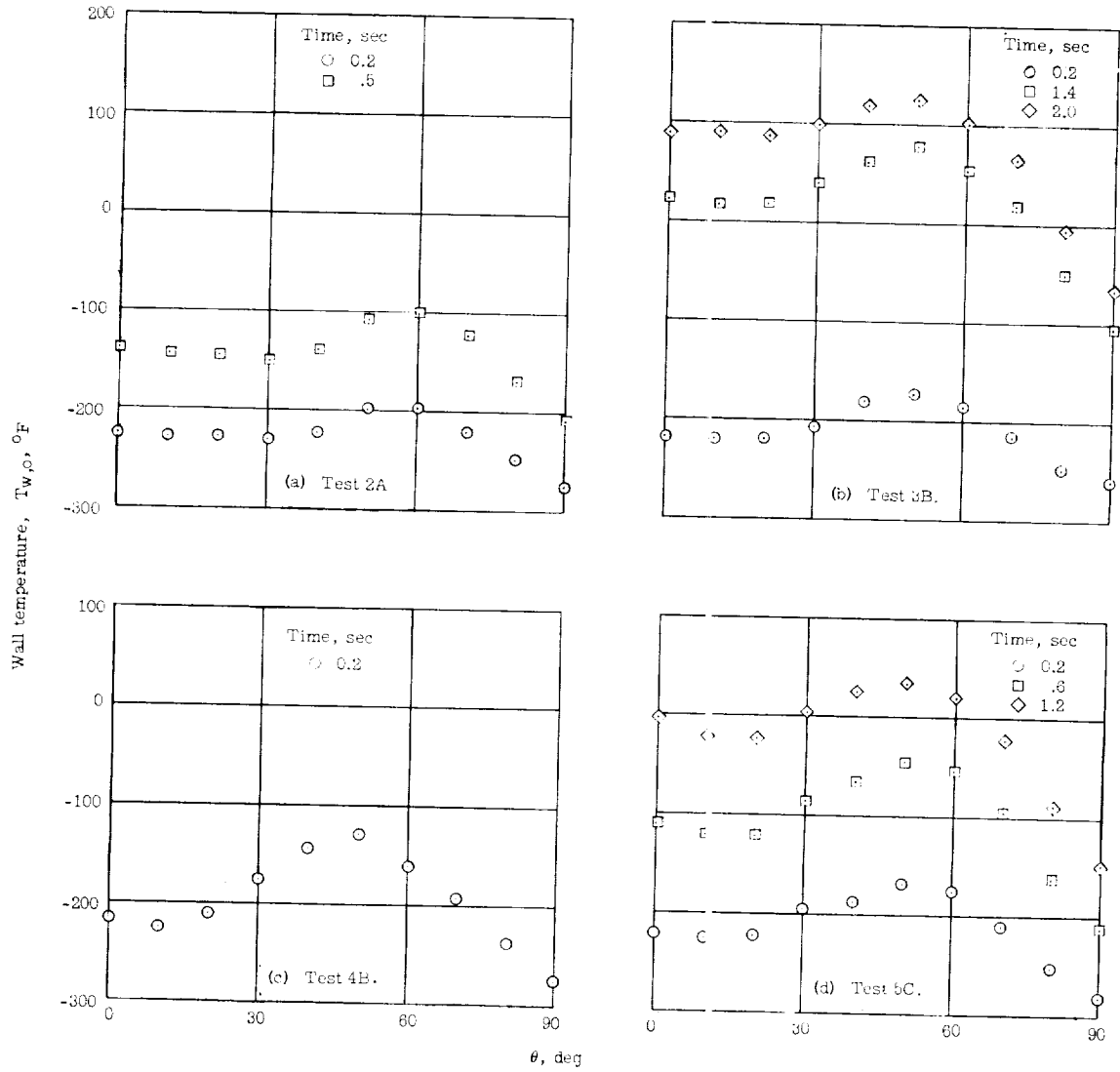
L-752

L-752

Figure 6.- Heat-transfer results. Hot wall; test 1A.

28

Figure 7.- Wall-temperature distributions. Cold wall; tests 2A, 3B, 4B, and 5C.
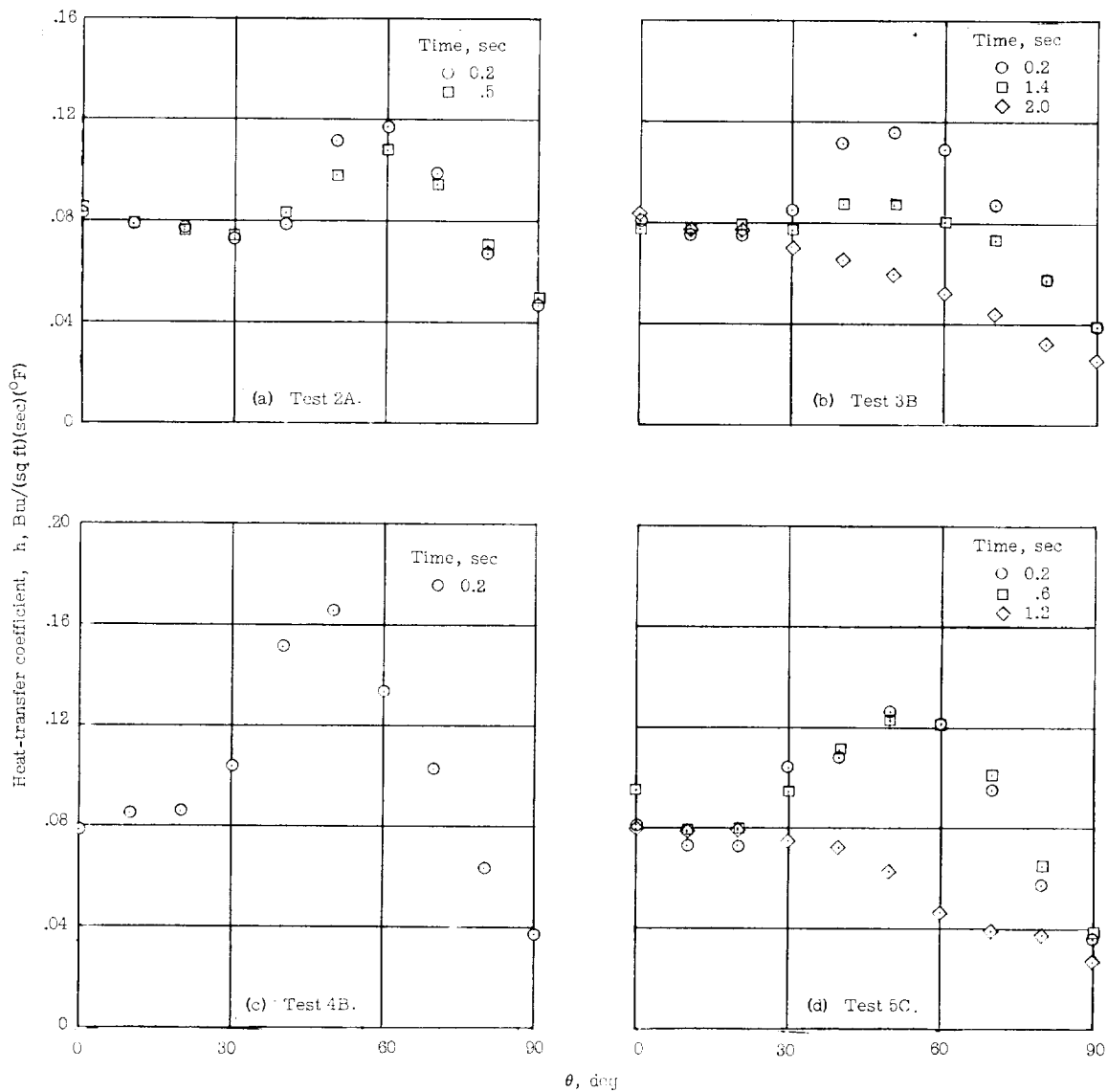
L-752

Figure 8.- Heat-transfer coefficients. Cold wall; tests 2A, 3B, 4B, and 5C.
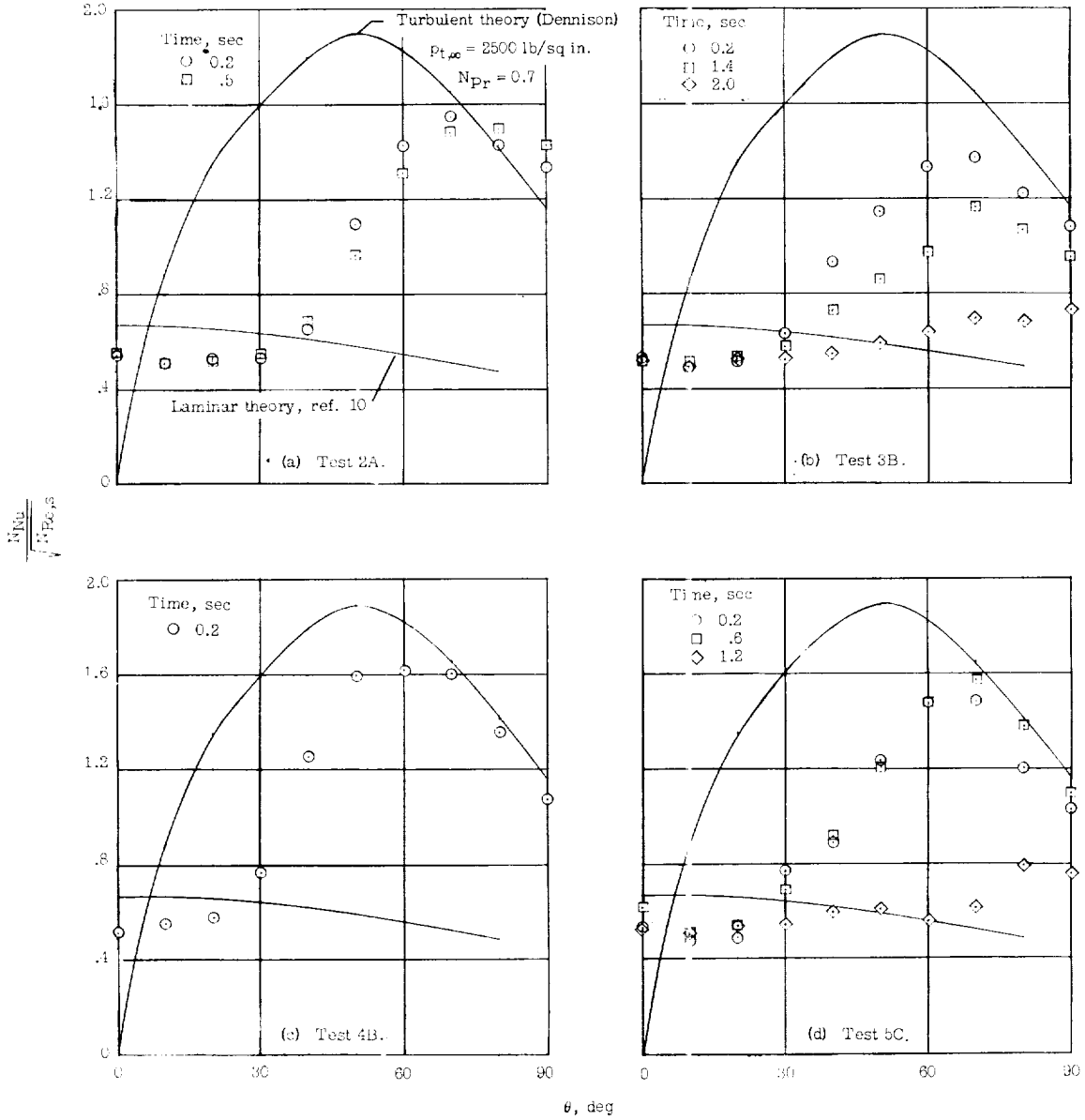
Figure 9.- Comparison of experimental and theoretical heat transfer. Cold wall; tests 2A, 3B, 4B, and 5C.
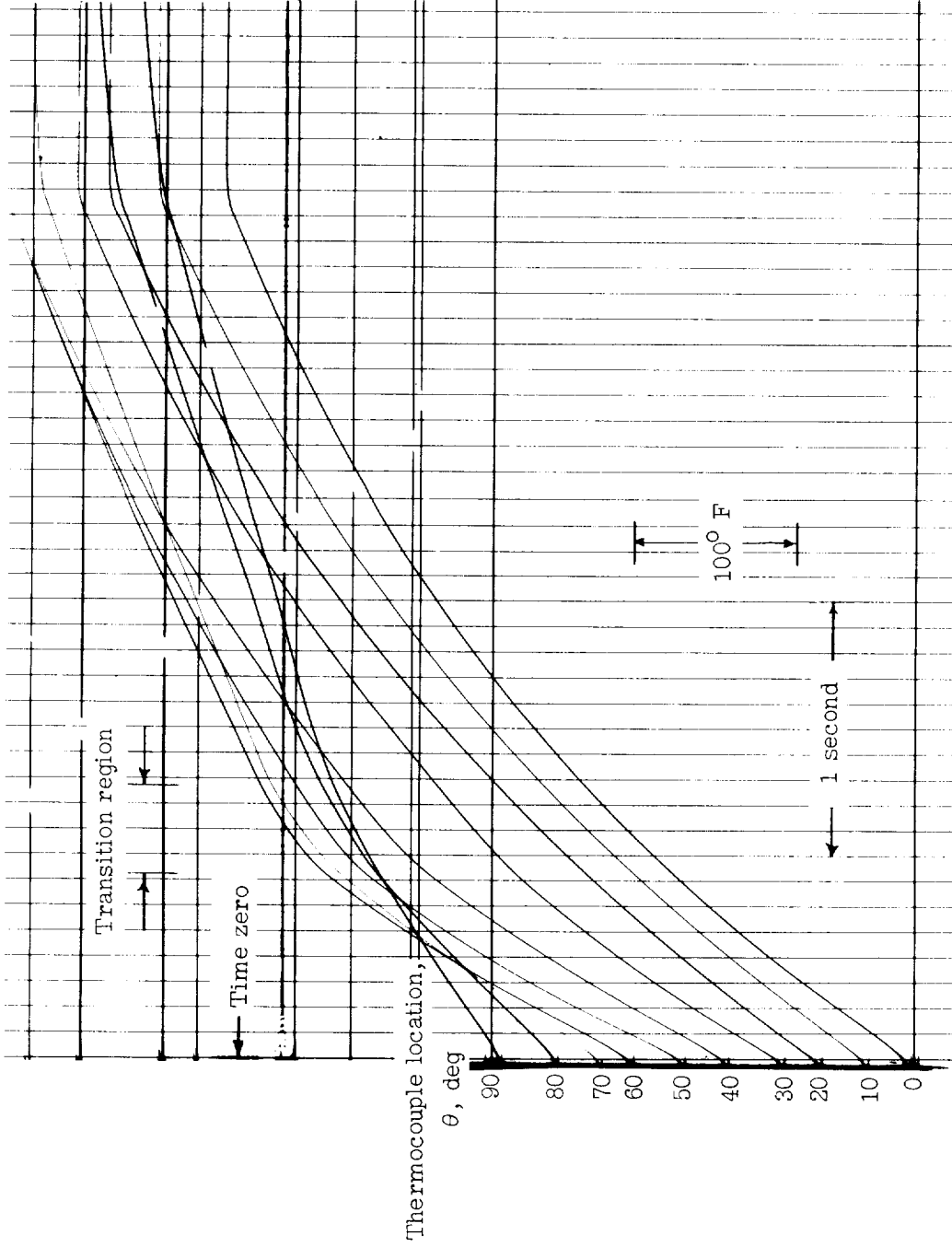
L-752

Figure 10.- Galvanometer record for test 5C.

Transiton time

Time zero

Thermocouple location,
θ, deg

90

80
70
60

50

40

30

20

10

0

100° F

1 second
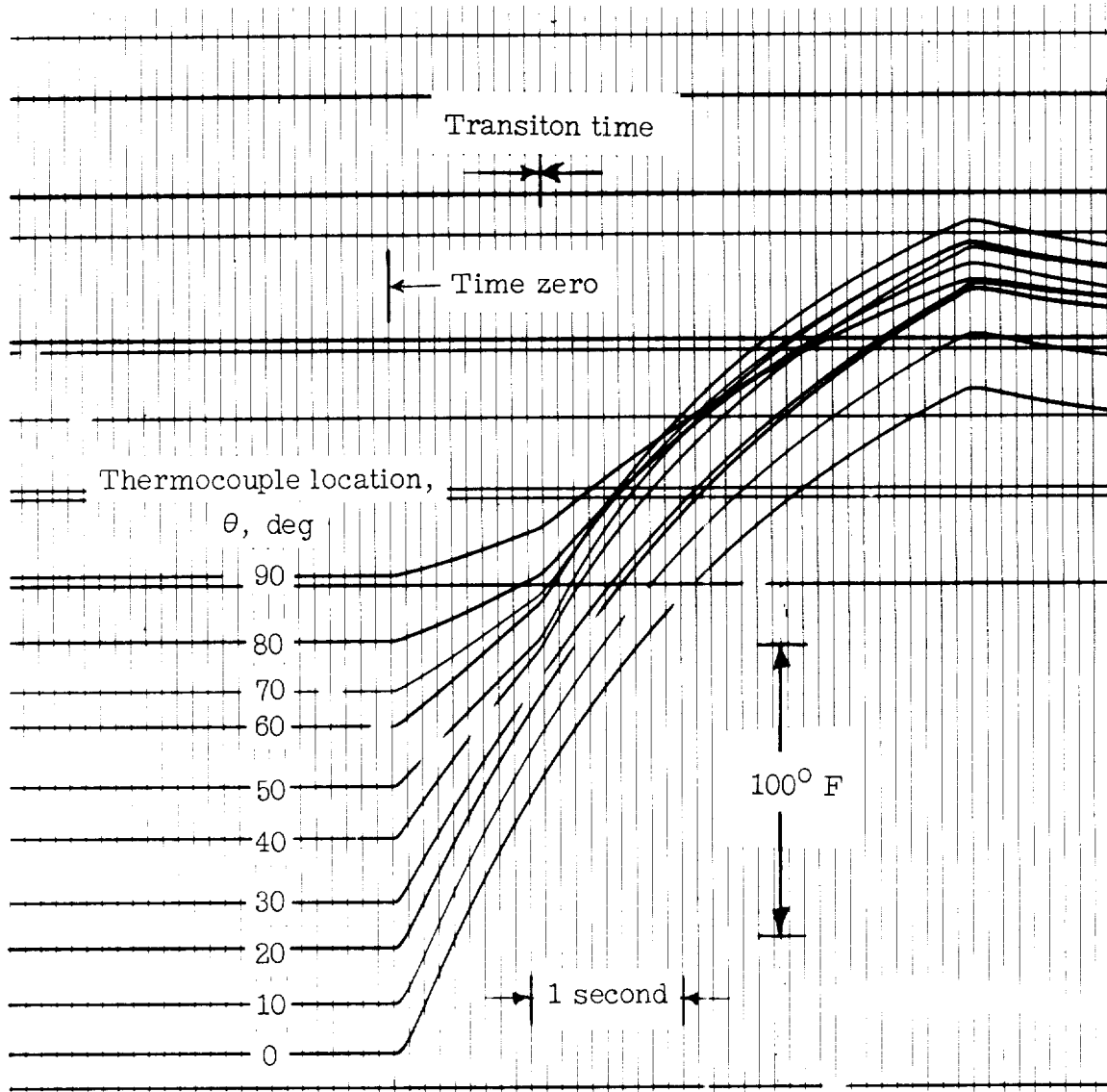
Figure 11.- Galvanometer record for test 1A.

L-752
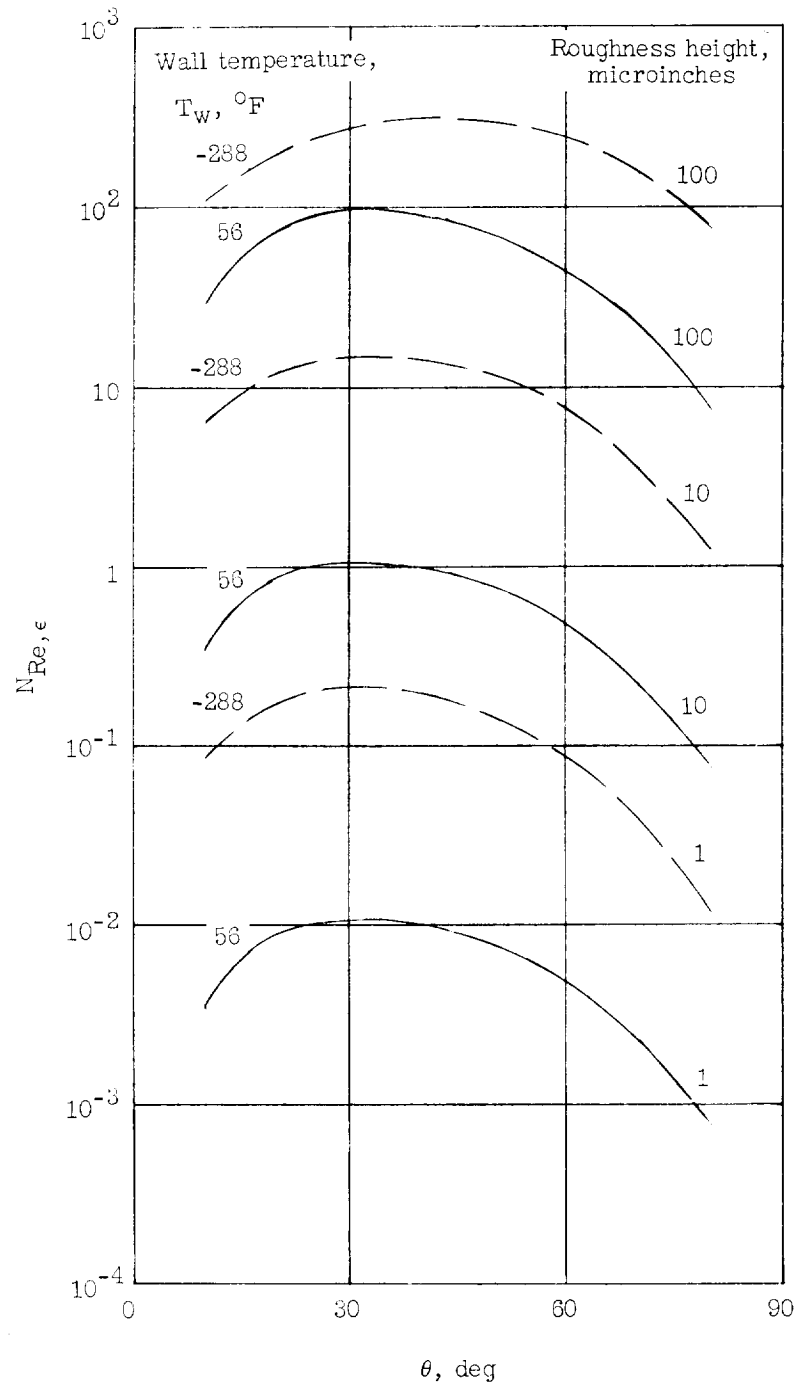
Figure 12.- Variation of roughness Reynolds number with angular
position, wall temperature, and roughness height. M = 4.95;
$p_{t,\infty}$ = 2,500 lb/sq in. abs; $T_{t,\infty}$ = 400° F.
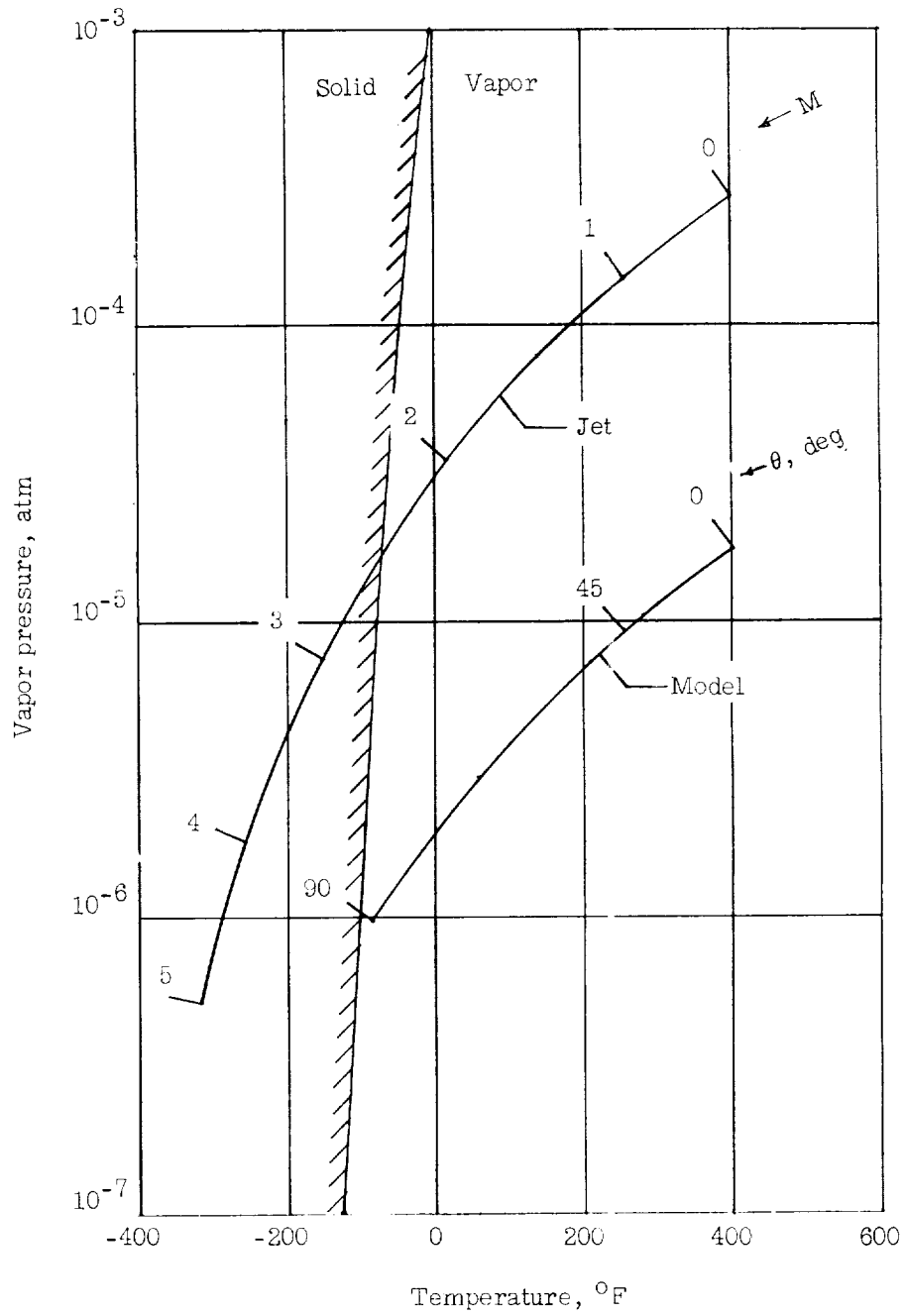
Figure 13.- Vapor pressure curve for ice around model (based on local conditions outside boundary layer) and in supersonic nozzle (based on local free-stream conditions). $p_{t,\infty}$ = 2,500 lb/sq in. abs; $T_{t,\infty}$ = 400° F; weight ratio of water to air, 10^{-6}.
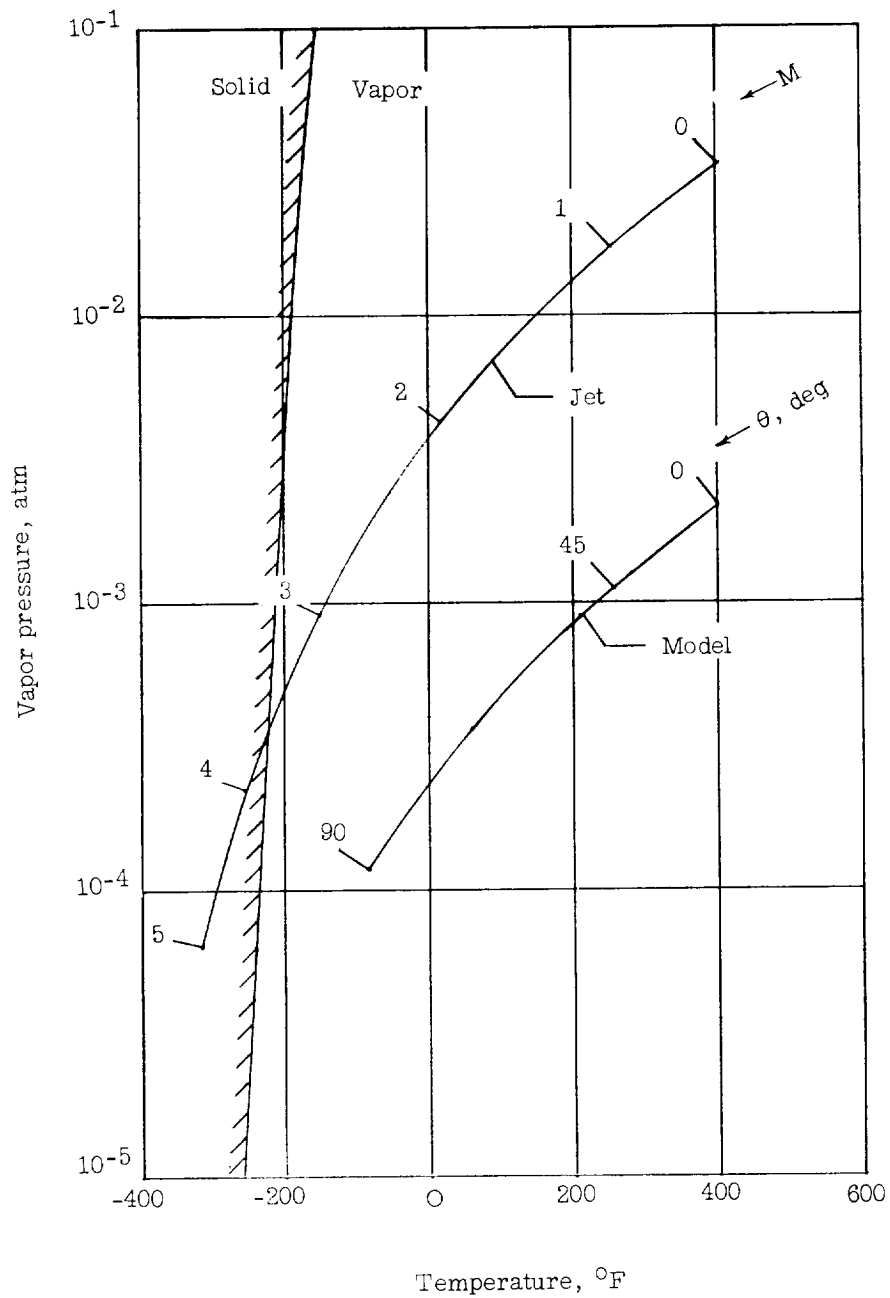
L-752

Figure 14.- Vapor pressure curve for solid carbon dioxide around model (based on local conditions outside boundary layer) and in supersonic nozzle (based on local free-stream conditions). $p_{t,\infty} = 2,500$ lb/sq in. abs; $T_{t,\infty} = 400^{\circ}$ F; weight ratio of carbon dioxide to air, 3×10^{-4}.
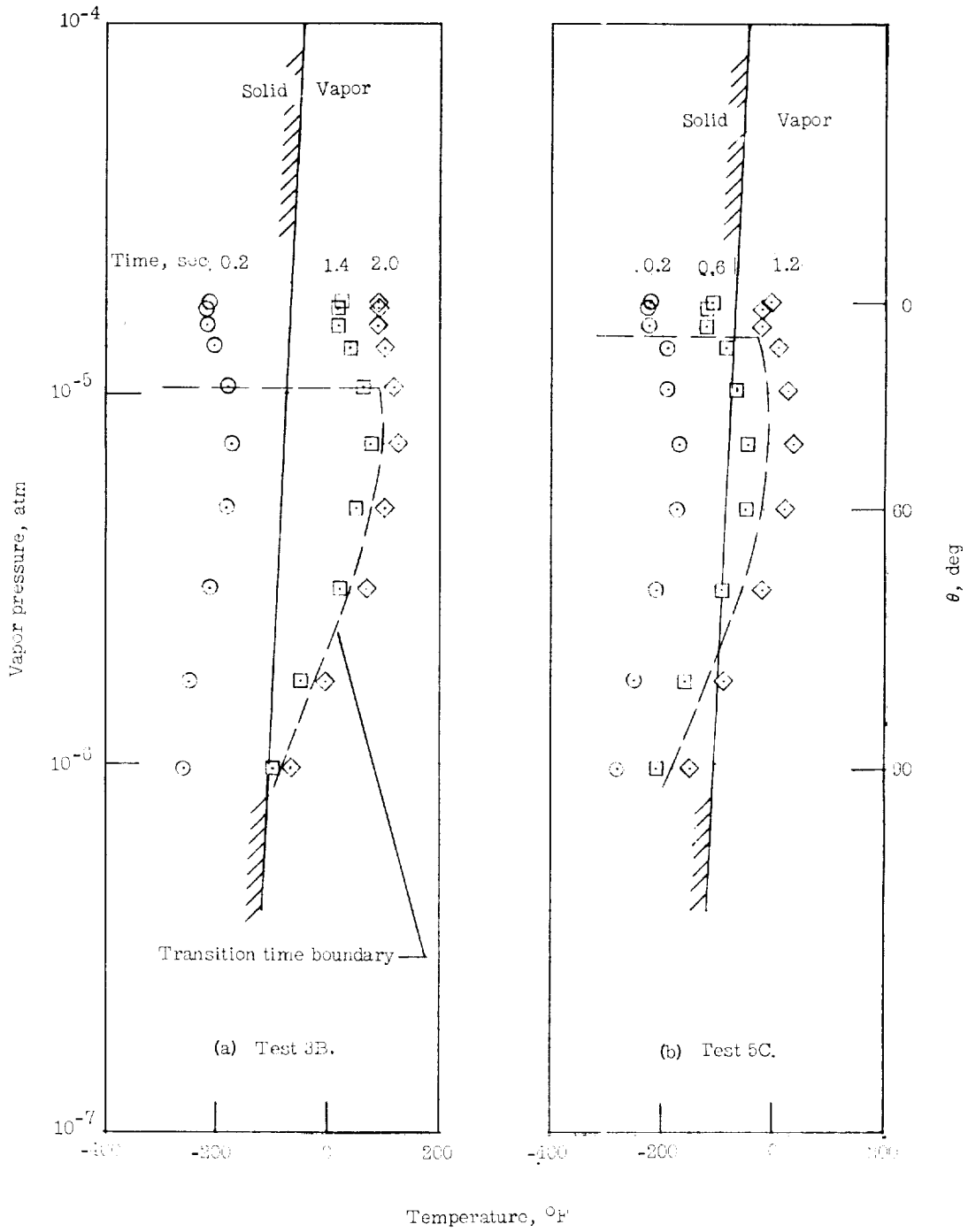
Figure 15.- Vapor pressure curves for ice around model. Data based on outside wall temperature and a weight ratio of water to air of 10^{-6}. $p_{t,\infty}$ = 2,500 lb/sq in. abs; $T_{t,\infty}$ = 400° F.
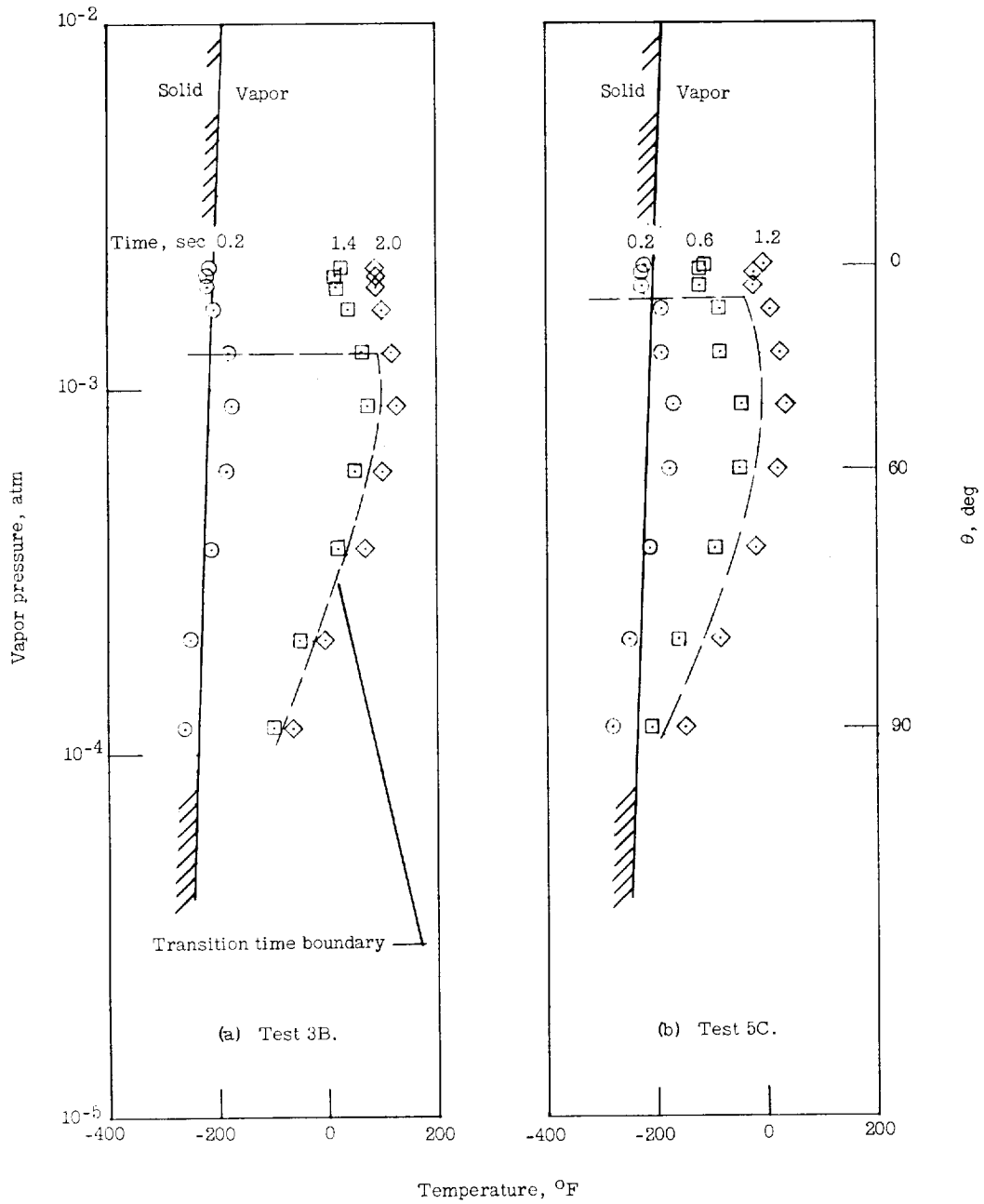
L-752

Figure 16.- Vapor pressure curves for solid carbon dioxide around model. Data based on outside wall temperature and a weight ratio of carbon dioxide to air of 3×10^{-4}. $p_{t,\infty} = 2,500$ lb/sq in. abs; $T_{t,\infty} = 400^\circ$ F.